

Status of Supersymmetric Seesaw in SO(10) models

L. Calibbi,¹ D. Chowdhury,² A. Masiero,³ K. M. Patel⁴ and S. K. Vempati²

¹*Max-Planck-Institut für Physik (Werner-Heisenberg-Institut), München 80805, Germany*

²*Centre for High Energy Physics, Indian Institute of Science, Bangalore 560 012, India*

³*INFN, Sezione di Padova and Dip. di Fisica ‘Galileo Galilei’, Univ. di Padova, Padova 35131, Italy*

⁴*Physical Research Laboratory, Navarangpura, Ahmedabad 380 009, India*

E-mail: calibbi@mppmu.mpg.de, debtosh@cts.iisc.ernet.in,
antonio.masiero@pd.infn.it, kmpatel@prl.res.in,
vempati@cts.iisc.ernet.in

ABSTRACT: We report on the status of supersymmetric seesaw models in the light of recent experimental results on $\mu \rightarrow e + \gamma$, θ_{13} and the light Higgs mass at the LHC. SO(10)-like relations are assumed for neutrino Dirac Yukawa couplings and two cases of mixing, one large, PMNS-like, and another small, CKM-like, are considered. It is shown that for the large mixing case, only a small range of parameter space with moderate $\tan \beta$ is still allowed. This remaining region can be ruled out by an order of magnitude improvement in the current limit on $\text{BR}(\mu \rightarrow e + \gamma)$. We also explore a model with non-universal Higgs mass boundary conditions at the high scale. It is shown that the renormalization group induced flavor violating slepton mass terms are highly sensitive to the Higgs boundary conditions. Depending on the choice of the parameters, they can either lead to strong enhancements or cancellations within the flavor violating terms. Such cancellations might relax the severe constraints imposed by lepton flavor violation compared to mSUGRA. Nevertheless for a large region of parameter space the predicted rates lie within the reach of future experiments once the light Higgs mass constraint is imposed. We also update the potential of the ongoing and future experimental searches for lepton flavor violation in constraining the supersymmetric parameter space.

Contents

1	Introduction	1
2	Seesaw in mSUGRA and NUHM	3
3	Parameter Range and Phenomenological Constraints	4
4	LFV in SUSY SO(10)	6
4.1	Combined effect of the Higgs mass and $\text{BR}(\mu \rightarrow e\gamma)$ bounds	10
5	Summary and Outlook	12
A	Description of Future Experiments and Prospects: Circa 2020	12

1 Introduction

Current times are unprecedented in terms of experimental activity in high energy physics. There have been several results of very high impact in the recent times. The following three are the most relevant for the purpose of our discussion.

- Firstly, LHC experiments have reported the discovery of a new boson with mass of about 125 GeV [1, 2], compatible with the Standard Model (SM) Higgs boson. In minimal supersymmetric standard model (MSSM), this would imply a mass of this order and SM-like couplings for the lightest CP-even Higgs boson [3–6]. In our analysis, we will take the 2σ mass range obtained in [3]

$$124.5 \text{ GeV} \lesssim m_h \lesssim 126.5 \text{ GeV}, \quad (1.1)$$

where m_h stands for the mass of the lightest neutral Higgs. In addition, LHC has also improved the limits on the spectrum of low-energy supersymmetry (SUSY) [7].

- The limit on the lepton flavor violating (LFV) decay $\mu \rightarrow e + \gamma$ has improved by one order of magnitude [8]. The current limit is

$$\text{BR}(\mu \rightarrow e + \gamma) < 2.4 \times 10^{-12} \text{ (90\% CL)}. \quad (1.2)$$

- Finally, the so-far unknown neutrino mixing angle, θ_{13} has been experimentally determined [9, 10]. The Daya Bay and RENO experiments have measured θ_{13} with very good accuracy:

$$\begin{aligned} \sin^2 2\theta_{13} &= 0.092 \pm 0.016(\text{stat.}) \pm 0.005(\text{syst.}) && \text{Daya Bay [9]} \\ \sin^2 2\theta_{13} &= 0.113 \pm 0.013(\text{stat.}) \pm 0.019(\text{syst.}) && \text{RENO [10]} \end{aligned} \quad (1.3)$$

The implications of the measurement of the light Higgs mass for various supersymmetric models have been studied in detail by various authors [11–23]. Supersymmetric seesaw models have not been explored so far in the light of these results¹. Furthermore, flavor violation is expected from SUSY seesaw models where the last two experimental results would play a crucial role in constraining the parameter space. In the present work, we consider the implications of all the three experimental results on a class of SUSY seesaw models inspired by SO(10) GUTs.

SO(10) GUT Models typically relate up-quark Yukawa matrices with the Dirac neutrino Yukawa couplings of the Type I seesaw mechanism. In fact, at least one of the neutrino Yukawa couplings is expected to be as large as the top Yukawa coupling, as a consequence of the underlying SO(10) symmetry [25]. Concerning the mixing structure of the neutrino Yukawa matrix, two extreme cases can be motivated by simple SO(10) models: large PMNS-like mixing or small CKM-like mixing. Lepton flavor violation in this class of models has been studied in Refs. [25–27]. The present work can be considered as an update of these studies.

The previous works considered mSUGRA/CMSSM-type boundary conditions for the SUSY-breaking soft terms. While universality of the soft terms at the GUT scale is required for the fields belonging to the same **16** representation of SO(10), the full universal boundary conditions of the CMSSM type are too strong a condition. For example, there is no fundamental reason why the Higgs doublets (that typically are in 10-dimensional representations) and the sfermion soft masses should be degenerate. Thus, strict universality between matter and Higgs fields can be relaxed [28]. These models are typically dubbed Non-Universal Higgs Mass models (NUHM). The relaxation of the universality has an important impact on the seesaw generated flavor violating entries of the slepton mass matrix. The magnitude of the RG generated flavor violating entries can either increase or decrease at the leading order due to the interplay between the matter and Higgs mass terms at the GUT scale. Cancellations in the flavor violating entry can indeed relax the LFV constraints on the SUSY parameter space. However, as we are going to see, the Higgs mass and LFV constraints are such that we have similar conclusions as in the mSUGRA, for moderate/large values of $\tan\beta$: an improvement of one order of magnitude in the $\text{BR}(\mu \rightarrow e + \gamma)$ bound is sufficient to rule out significant amount of the parameter space. In the present work, we compare and contrast the constraints on SUSY seesaw parameter space with CMSSM/mSUGRA boundary conditions and NUHM boundary conditions.

We find that in the PMNS case, $\tan\beta$ is restricted between 4 to 20. Lower values of $\tan\beta$ are disfavored by the light Higgs mass constraints whereas higher values are strongly constrained by the present limit on $\text{BR}(\mu \rightarrow e + \gamma)$ whose rates can be very large, as a consequence of the sizable observed value of θ_{13} . Furthermore, the one order of magnitude improvement expected in the near future from the MEG experiment would rule out most of the SUSY parameter space accessible at the LHC. This situation is somewhat relaxed in the NUHM model where we considered the masses of both the Higgs doublets to be the same (the so-called NUHM1 model). We have further updated the future prospects for both the CKM and PMNS cases in mSUGRA/CMSSM as well as in NUHM1.

The paper is organized as follows. In section 2, we recap the SUSY seesaw and discuss the generation of flavor violation in mSUGRA and NUHM1. In section 3, we discuss the

¹As this work was finished and being prepared for submission, the following paper Ref.[24] appeared on arXiv.

details of our numerical analysis. In section 4, we present our results. We conclude with a summary and outlook in section 5. Finally, in appendix A we describe the proposed future experiments and their expected sensitivity.

2 Seesaw in mSUGRA and NUHM

The phenomenology of SUSY Type I seesaw mechanism with universal boundary conditions (mSUGRA/CMSSM) has been studied in many papers (see [29, 30] for a set of recent works). Here we review some essential features related to flavor violation for completeness and to do a comparison with the case of non-universal Higgs masses. To set the notation, the Type I seesaw mechanism is characterized by a superpotential containing the following terms

$$\mathcal{W} \supset \mathbf{Y}_e L e^c H_d + \mathbf{Y}_\nu L \nu^c H_u + \frac{1}{2} M_R \nu^c \nu^c \quad (2.1)$$

where L (e^c) stands for the leptonic doublets (singlets) and ν^c are the right-handed (RH) neutrino superfields (with the generation indices not explicitly written). \mathbf{Y}_e and \mathbf{Y}_ν are the electron and neutrino (Dirac) Yukawa matrices.

In models like CMSSM/mSUGRA, the soft terms are assumed to be universal at the Grand Unification (GUT) scale, $M_{\text{GUT}} \sim 2 \times 10^{16}$ GeV. At the weak scale as is well known, the soft terms are no longer universal due to the effects of the renormalization group (RG) running. The presence of the RH neutrinos of eq. (2.1) at an intermediate scale contribute to the running and generate flavor violating entries in the left-handed slepton mass matrix at the weak scale [31]. At the leading order these terms can be estimated to be:

$$(m_L^2)_{i \neq j} \equiv (\Delta_{i \neq j}^\ell)_{LL} \approx -\frac{3m_0^2 + A_0^2}{8\pi^2} \sum_k (Y_\nu^*)_{ik} (Y_\nu)_{jk} \log \left(\frac{M_X}{M_{R_k}} \right), \quad (2.2)$$

where M_X represents the GUT scale and M_{R_k} , the scale of the k^{th} RH neutrino. m_0 and A_0 stand for the usual universal soft mass and trilinear terms at the high scale. \mathbf{Y}_ν , the Dirac neutrino Yukawa couplings are free parameters in the Type I seesaw mechanism which cannot be completely determined even after including the complete data on the neutrino mass matrix [32].

SO(10) models with their matter representations being 16-dimensional provide a natural setting for the seesaw mechanisms. Furthermore, they provide information about the neutrino Yukawa couplings. For example, it is known that as long as we restrict to renormalisable SO(10) models, at least one of the neutrino Yukawa couplings should be as large as the top Yukawa coupling [25]. Thus with suitable assumptions for the (left-handed) mixing of the Dirac Yukawa Neutrino mass matrix, one can make predictions for the flavor violation generated at the weak scale from eq. (2.2). Two extreme scenarios for mixing are typically considered to be present in \mathbf{Y}_ν [25, 26, 33] :

$$\begin{aligned} \mathbf{Y}_\nu &= \mathbf{Y}_u && \text{(CKM Case)} \\ \mathbf{Y}_\nu &= \mathbf{Y}_u^{\text{diag}} \mathbf{U}_{\text{PMNS}} && \text{(PMNS Case),} \end{aligned} \quad (2.3)$$

where $\mathbf{Y}_u = \mathbf{V}_{\text{CKM}} \mathbf{Y}_u^{\text{diag}} \mathbf{V}_{\text{CKM}}^\dagger$. Both these scenarios can be motivated from concrete models of fermion masses within the SO(10) framework [25, 26]. The flavor violating off-diagonal entries at the weak scale, eq. (2.2), are then completely determined by assuming

Generations	PMNS	CKM
Δ_{12}	$Y_t^2 U_{e3} U_{\mu 3}$	$Y_t^2 V_{td} V_{ts}$
Δ_{23}	$Y_t^2 U_{\mu 3} U_{\tau 3}$	$Y_t^2 V_{tb} V_{ts}$
Δ_{31}	$Y_t^2 U_{e3} U_{\tau 3}$	$Y_t^2 V_{td} V_{tb}$

Table 1. The dominant combination of neutrino Yukawa couplings which enter eq. (2.2) in CKM and PMNS mixing case.

\mathbf{Y}_ν as in eq. (2.3). The dominant combinations of Yukawa couplings which enter the radiative generation of $(\Delta_{i \neq j}^\ell)_{LL}$ are shown in table (1). Notice that the hierarchical structure of \mathbf{Y}_ν dictated by SO(10) determines that the leading contribution corresponds to third generation particles running in the loop. Hence, the flavor violating entries $(\Delta_{12})_{LL}$ responsible for $\mu \rightarrow e\gamma$ process and $(\Delta_{13})_{LL}$ responsible for $\tau \rightarrow e\gamma$ depend on $U_{e3} \sim \theta_{13}$ in the PMNS case. The branching ratios of the LFV decays can be roughly estimated to be

$$\frac{\text{BR}(l_i \rightarrow l_j \gamma)}{\text{BR}(l_i \rightarrow l_j \nu \bar{\nu})} \approx \frac{\alpha^3}{G_F^2} \frac{(\delta_{LL})_{ij}^2}{m_{\text{susy}}^4} \tan^2 \beta \quad (2.4)$$

where m_{susy} is a typical SUSY mass and the flavor violation is as usual parameterize by the following quantity

$$\delta_{ij}^f \equiv \frac{\Delta_{ij}^f}{m_f^2}. \quad (2.5)$$

Let us now turn our attention to the NUHM1 boundary conditions.² At the first sight one might expect that such a modification has no significant effect on the LFV amplitudes, except for those due to the modifications in the sparticle spectrum. However, it turns out that this is not the only modification. The flavor mixing structure of the slepton mass matrix can also be strongly affected. The radiatively generated flavor violating entries in eq. (2.2) take the following form in NUHM models:

$$(\Delta_{i \neq j}^\ell)_{LL} \approx -\frac{2m_0^2 + m_{H_u}^2 + A_0^2}{8\pi^2} \sum_k (Y_\nu^*)_{ik} (Y_\nu)_{jk} \log \left(\frac{M_X}{M_{R_k}} \right), \quad (2.6)$$

where m_{H_u} is the soft mass of the up-type Higgs at the high scale. In the present work, we consider the NUHM1 scenario, i.e. $m_{H_u} = m_{H_d}$ at the GUT scale. Furthermore, there can be a relative sign difference between the universal mass terms for the matter fields (that we still call m_0 with abuse of notation) and the Higgs mass terms at the GUT scale. This can clearly lead to cancellations (for $m_{H_u}^2 \approx -2 m_0^2$) or enhancements (for $m_{H_u}^2 \gtrsim m_0^2$) in the magnitude of the flavor violating entries at the weak scale compared to mSUGRA.

3 Parameter Range and Phenomenological Constraints

As mentioned earlier, we will consider two sets of boundary conditions for the soft-terms in our numerical analysis. While the mSUGRA is characterized by the standard ‘four

²Lepton flavor violation in NUHM models has been previously studied in [34], where correlations between $\mu \rightarrow e + \gamma$ and $\mu \rightarrow e$ conversion rates have been discussed.

and half' parameters ($m_0, M_{1/2}, A_0, \tan \beta, \text{sgn}(\mu)$), we parametrize the NUHM1 case by $m_{H_u} = m_{H_d} \equiv m_0 - \Delta m_H$. Considering the present and future LHC accessible regions as well as the reach of future flavor physics experiments, we scan the soft parameter space in the following ranges:

$$\begin{aligned}
m_0 &\in [0, 5] \text{ TeV} \\
\Delta m_H &\in \begin{cases} 0 & \text{for mSUGRA} \\ [0, 5] & \text{for NUHM1} \end{cases} \\
m_{1/2} &\in [0.1, 2] \text{ TeV} \\
A_0 &\in [-3m_0, +3m_0] \\
\text{sgn}(\mu) &\in \{-, +\}
\end{aligned} \tag{3.1}$$

Note that we use the convention in which $m_{H_u}^2 = \text{sgn}(m_{H_u}) |m_{H_u}|^2$. For this range of the parameter space the first two generations squarks have masses up to $m_{\tilde{q}_{1,2}} \simeq 7$ TeV and the first two generations sleptons up to $m_{\tilde{\ell}_{1,2}} \simeq 5$ TeV. We include in our scan such spectra beyond the reach of direct SUSY searches at the LHC, in order to check the capability of the flavor violating observables in constraining the parameter space.

The numerical analysis is carried out using the SUSEFLAV package [35]. It evaluates 2-loop MSSM RGEs with full 3×3 flavor mixing effects and also incorporates one-loop SUSY threshold corrections in all the MSSM parameters. It checks for consistent Radiative Electroweak Symmetry Breaking (REWSB) by minimizing the one-loop corrected effective superpotential. The program incorporates the effect of RH neutrinos on MSSM RGEs and calculates the branching ratios of various LFV processes induced by such RGE effects. The program also calculates $\text{BR}(b \rightarrow s\gamma)$ in the minimal flavor violation assumptions. We also calculate the $\text{BR}(B_s \rightarrow \mu^+ \mu^-)$ using ISABMM subroutine of ISAJET [36]. The light Higgs mass is computed using the full two loop corrections of [37–40]. First, we collect the points which (a) successfully give REWSB, (b) have no any tachyonic sfermions at the weak scale and (c) have the lightest neutralino as Lightest Supersymmetric Particle (LSP). Then we calculate all the LFV observables, $\text{BR}(b \rightarrow s\gamma)$ using the SUSY spectrum evaluated for each point. Finally, we impose the following experimental constraints on the data points we collected.

$$\begin{aligned}
121.5 \text{ GeV} &\leq m_h \leq 129.5 \text{ GeV} \\
m_{\tilde{\chi}^\pm} \text{ (lightest Chargino mass)} &\geq 103.5 \text{ GeV} \quad [41] \\
\text{BR}(B_s \rightarrow \mu^+ \mu^-) &< 4.5 \times 10^{-9} \quad [42] \\
2.85 \times 10^{-4} &\leq \text{BR}(b \rightarrow s\gamma) \leq 4.24 \times 10^{-4} \quad (2\sigma)[43].
\end{aligned} \tag{3.2}$$

In comparing our predictions for m_h with the experimental range of eq.(1.1), we take into account 3 GeV of theoretical uncertainty (for a recent discussion see [44]). We have not considered the Supersymmetric solution to $(g - 2)_\mu$ discrepancy in the present work.

In our study, we assume normal hierarchy in the light neutrino mass spectrum and set

$$m_{\nu_1} = 0.001 \text{ eV}, \quad m_{\nu_2} = \sqrt{\Delta m_{\text{sol}}^2 + m_{\nu_1}^2} \text{ and } m_{\nu_3} = \sqrt{\Delta m_{\text{atm}}^2 + m_{\nu_1}^2} \tag{3.3}$$

LFV Process	Present bound	Near future sensitivity of ongoing experiments
BR($\mu \rightarrow e\gamma$)	2.4×10^{-12} [8]	10^{-13} [45]
BR($\mu \rightarrow eee$)	1.0×10^{-12} [46]	—
CR($\mu \rightarrow e$ in Ti)	4.3×10^{-12} [47]	—
BR($\tau \rightarrow e\gamma$)	3.0×10^{-8} [43]	—
BR($\tau \rightarrow eee$)	3.0×10^{-8} [43]	—
BR($\tau \rightarrow \mu\gamma$)	4.5×10^{-8} [43]	10^{-8} [45]
BR($\tau \rightarrow \mu\mu\mu$)	2.0×10^{-8} [43]	3×10^{-9} [45]

Table 2. Present bounds and expected sensitivities on LFV processes.

where Δm_{sol}^2 and Δm_{atm}^2 are the solar and atmospheric squared mass differences respectively and we use the central values obtained from recent global fits on neutrino data [48]:

$$\Delta m_{\text{sol}}^2 = 7.62 \times 10^{-5} \text{ eV}^2 \text{ and } \Delta m_{\text{atm}}^2 = 2.53 \times 10^{-3} \text{ eV}^2 \quad (3.4)$$

Regarding the mixing angles, we take the most conservative value for the reactor mixing angle and set $|U_{e3}| = 0.11$, that corresponds to the lower limit of the 3σ range given by RENO [10] as well as by the global fits [48]. The remaining two angles of the PMNS matrix are set to their global fit values $\theta_{12} = 33.5^\circ$ and $\theta_{23} = 45^\circ$. The masses of heavy neutrinos which we use in our analysis are:

$$M_{R_1} = 10^6 \text{ GeV}, \quad M_{R_2} = 10^9 \text{ GeV}, \quad \text{and} \quad M_{R_3} = 10^{14} \text{ GeV}. \quad (3.5)$$

The recent results from the MEG collaboration [8] have improved the existing bound on BR($\mu \rightarrow e\gamma$) by one order of magnitude. The present limits on different LFV observables are summarized in table 2. In the following subsections, we discuss in detail the results of numerical analysis carried out in the PMNS and CKM cases with mSUGRA and NUHM1 boundary conditions and present a quantitative comparisons between them.

4 LFV in SUSY SO(10)

Let us start considering the PMNS case, where there is a direct link between LFV processes and neutrino parameters. Besides the CP violating phases, θ_{13} was the only unknown parameter in the leptonic mixing sector till some time ago. There have been various theoretical models based on the idea that θ_{13} could be very small, close to zero. In such a case, the resulting $\mu \rightarrow e + \gamma$ and $\tau \rightarrow e + \gamma$ rates could have been suppressed [49, 50]. Recent experiments prove the contrary. Both the experiments measuring θ_{13} are in good agreement with each other and indicate a sizeable value of θ_{13} . The recent global fit analysis [48] also leads to similar value of θ_{13} . All these results indicate that the smallest value of $|U_{e3}|$ is 0.11 at 3σ . The resulting rates of BR($\mu \rightarrow e\gamma$) are significantly enhanced for such a value of $|U_{e3}|$. As we are going to see, the updated MEG limit together with a large θ_{13} puts significant constraints on mSUGRA for moderate as well as large value of $\tan \beta$.³

³The interplay between large θ_{13} and BR($\mu \rightarrow e\gamma$) in the context of discrete flavor groups have been recently discussed in [51].

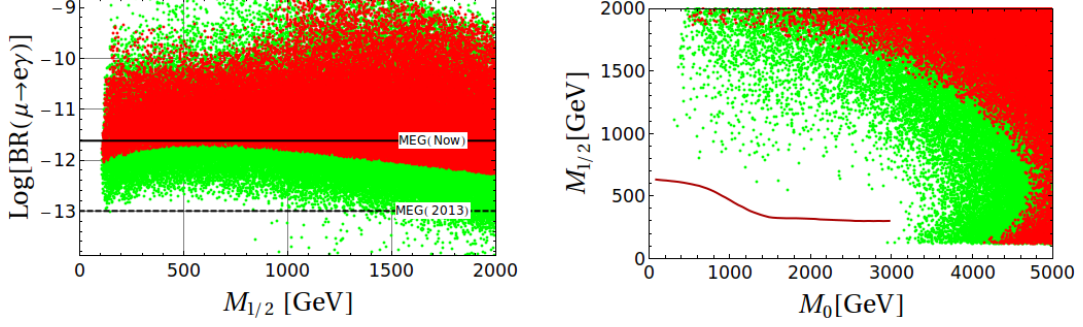


Figure 1. The figure in the left panel shows the $\text{BR}(\mu \rightarrow e\gamma)$ obtained by scanning the mSUGRA (in red color) and NUHM (in green color) parameters in the ranges given in eq. (3.1) and for fixed $\tan\beta = 10$ and $U_{e3} = 0.11$ (the lowest value allowed at 3σ by recent RENO observation) and satisfy all the constraints in eq. (3.2). Different horizontal lines correspond to present and future bounds on $\text{BR}(\mu \rightarrow e\gamma)$. The figure in the right panel shows the allowed space in the $m_0 - m_{1/2}$ plane which satisfy the current MEG bound and eq. (3.2). The region below the red line is excluded by the direct searches for SUSY at the LHC [7].

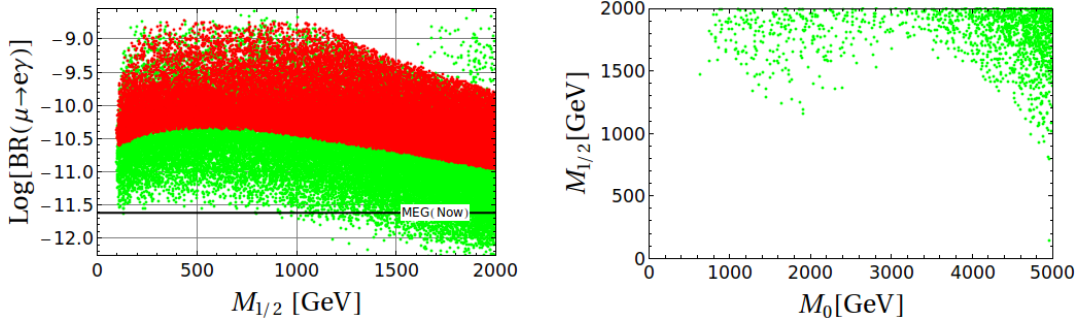


Figure 2. The same as figure 1 for $\tan\beta = 40$.

In figures 1 and 2 we present the constraints from $\text{BR}(\mu \rightarrow e\gamma)$ on mSUGRA and NUHM1 parameter space for $\tan\beta = 10$ and 40 respectively. As can be seen, while only small part of the parameter space survives for $\tan\beta = 10$ in mSUGRA, it is completely ruled out for $\tan\beta = 40$. The allowed regions for low $\tan\beta$ require very heavy spectra, i.e. $m_0 \gtrsim 4$ TeV for small $M_{1/2}$ or $M_{1/2} \gtrsim 2$ TeV for small m_0 . What is surprising is that the constraint on the NUHM1 parameter space is not as weak as one might expect from eq. (2.6). As we can see from the figures even in the presence of partial cancellations, most of the NUHM1 parameter space is going to be explored by MEG. If one removes the light Higgs mass constraint, points with stronger cancellations would be allowed, even with $\mu \rightarrow e\gamma$ rates below the MEG sensitivity. Thus points compatible with the Higgs mass bound, eq. (3.2), do not allow strong cancellations in the flavor violating entry in eq. (2.6). For the large $\tan\beta$ case, the $\mu \rightarrow e\gamma$ constraint is so strong that only few points with $M_{1/2} \gtrsim 800$ GeV are allowed. In the section 4.1, we will discuss in more detail about the impact of the constraint on m_h in mSUGRA and NUHM1.

In the context of the updated MEG limit on $\text{BR}(\mu \rightarrow e\gamma)$, it is now worthwhile to see what is the situation with the small mixing CKM case. Here we compare the CKM case and the PMNS case with mSUGRA boundary conditions. As above, red points correspond to the PMNS case while we use the blue color for CKM case. The CKM case has highly

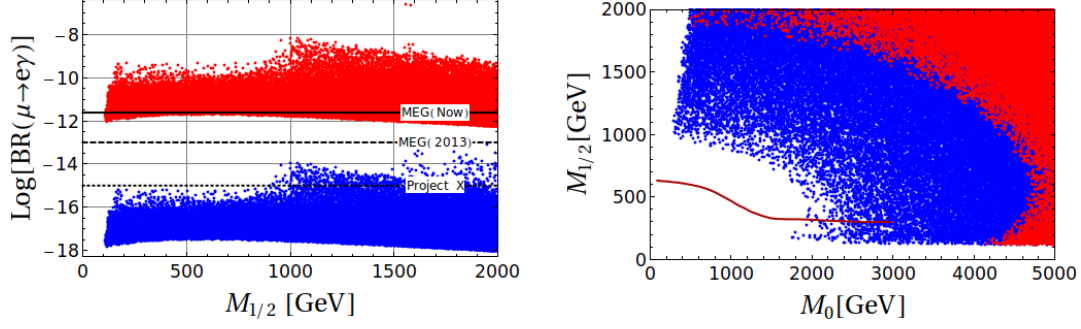


Figure 3. The figure in the left panel shows the $\text{BR}(\mu \rightarrow e\gamma)$ obtained by scanning the mSUGRA parameters in the ranges given in eq. (3.1) and for fixed $\tan \beta = 10$ and $U_{e3} = 0.11$ (the lowest value allowed at 3σ by recent RENO observation). The red (blue) colored points correspond to PMNS (CKM) case. Different horizontal lines correspond to present and future bounds on $\text{BR}(\mu \rightarrow e\gamma)$. The figure in the right panel shows the allowed space in the $m_0 - m_{1/2}$ plane which satisfy the current MEG bound. The region below the red line is excluded by the current LHC searches [7]. Both the plots satisfy all the constraints in eq. (3.2).

suppressed branching fractions due to the smallness of CKM angles (see table (1)) as has been detailed in [26]. Though there has been no strong improvements in the experimental sensitivity compared to the analyses of [26], we update the result with the light Higgs mass constraint. In figure 3 we show the results for $\tan \beta = 10$. As we can see, some part of the parameter space of the CKM case can be probed by the proposed Project-X experiment⁴ for $\mu \rightarrow e\gamma$. At present the main constraint to this scenario is simply provided by the m_h range of eq. (1.1), that excludes the regions with lighter SUSY spectra: $m_0 \lesssim 2$ TeV for small $M_{1/2}$, $M_{1/2} \lesssim 1$ TeV for small m_0 , as we can see from the right panel of the figure. We can also notice that the LHC limits on the mSUGRA parameter space has already started to constrain regions of the parameter space otherwise allowed by the bounds in eq. (3.2).

Let us now turn our attention to other observables like $\mu \rightarrow eee$, $\mu \rightarrow e$ conversion in nuclei and $\tau \rightarrow \mu\gamma$, which is independent of θ_{13} . In figures 4, 5 and 6, we show the predicted rates for $\tau \rightarrow \mu\gamma$, $\mu \rightarrow eee$ and $\mu \rightarrow e$ conversion in the Titanium nucleus versus the $\text{BR}(\mu \rightarrow e\gamma)$ (that is at present the most constraining LFV observable), for the PMNS case in mSUGRA (red points) and in NUHM1 (green points) as well as for the CKM case (blue points).

As can be seen from figure 4, in the PMNS case, the present MEG limit on $\text{BR}(\mu \rightarrow e\gamma)$ implies $\text{BR}(\tau \rightarrow \mu\gamma) \lesssim 10^{-12}$, beyond the reach of the proposed experiments. This is a direct consequence of the large value of θ_{13} measured by Daya Bay and RENO. In fact, from eq.(2.4,2.5) and table 1, we have:

$$\frac{\text{BR}(\tau \rightarrow \mu\gamma)}{\text{BR}(\mu \rightarrow e\gamma)} \approx \frac{|U_{\tau 3} U_{\mu 3}|^2}{|U_{\mu 3} U_{e 3}|^2} \times \text{BR}(\tau \rightarrow \mu\nu\bar{\nu}) \approx \mathcal{O}(1). \quad (4.1)$$

In the CKM case (blue points), the small mixing angle and the m_h bound are such that $\text{BR}(\tau \rightarrow \mu\gamma) \lesssim 10^{-10}$. Thus, the scenarios discussed here allow possible signals of LFV in

⁴In appendix A we present a brief summary of all the future experimental facilities related to the flavor violating observables discussed in the text.

$\mu - e$ transition only and evidence for $\text{BR}(\tau \rightarrow \mu\gamma)$ at future experiments would strongly disfavor them.

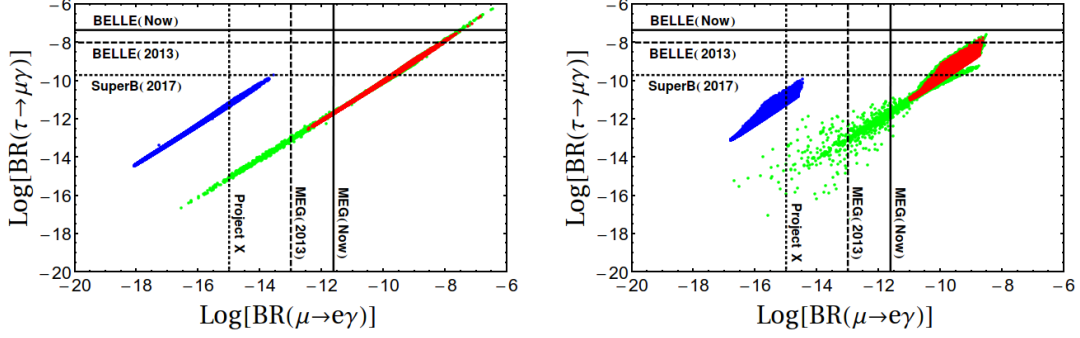


Figure 4. $\text{BR}(\tau \rightarrow \mu\gamma)$ versus $\text{BR}(\mu \rightarrow e\gamma)$ for the PMNS case in mSUGRA (red) and NUHM (green), and for the CKM case (blue) for $\tan\beta=10$ (left), for $\tan\beta=40$ (right). The different horizontal and vertical lines correspond to present and future limits on the respective observables.

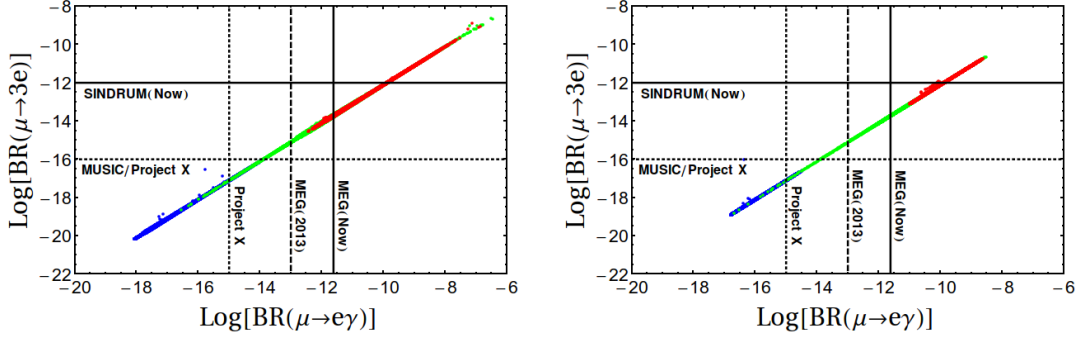


Figure 5. $\text{BR}(\mu \rightarrow eee)$ versus $\text{BR}(\mu \rightarrow e\gamma)$ for the PMNS case in mSUGRA (red) and NUHM (green), and for the CKM case (blue) for $\tan\beta=10$ (left), for $\tan\beta=40$ (right). The different horizontal and vertical lines correspond to present and future limits on the respective observables.

Let us now consider the decay $\mu \rightarrow eee$. It is known (see e.g. [52]) that in SUSY (with conserved R-parity) the dominant contribution to this process arises from the same dipole operator responsible for $\mu \rightarrow e\gamma$, hence the correlation of the two processes is striking:

$$\text{BR}(\mu \rightarrow eee) \sim \alpha_{\text{em}} \times \text{BR}(\mu \rightarrow e\gamma). \quad (4.2)$$

Such prediction is consistent with our results shown in figure 5 for $\tan\beta = 10$ and 40. The present bound on $\mu \rightarrow eee$ comes from the SINDRUM experiment at PSI. At present, MEG sets a stronger bound, as expected. However the future sensitivity reach of MUSIC and Project-X experiments will be able to go beyond the reach of MEG, testing most of the NUHM parameter space of our scan.

Let us now discuss $\mu \rightarrow e$ conversion in Nuclei, that will represent one of the most important probes of LFV in the future. Project X and J-PARC are envisaging facilities where μ conversion on various Nuclei can be studied (for a review, please see [53]). In the

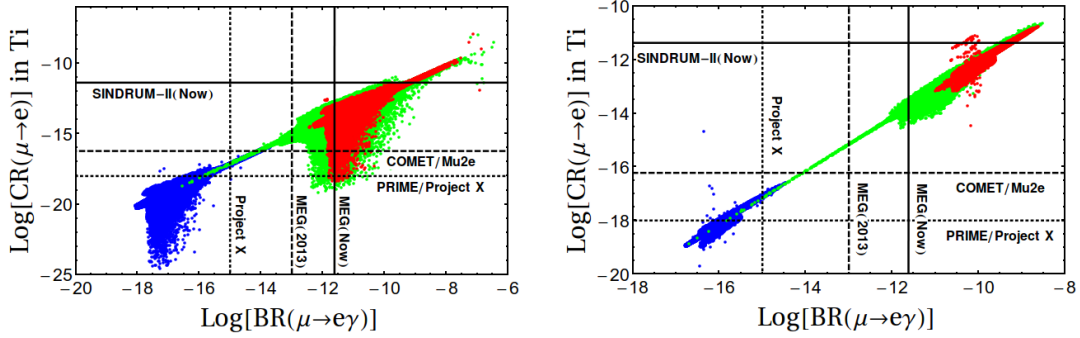


Figure 6. $\text{CR}(\mu \rightarrow e \text{ in Ti})$ versus $\text{BR}(\mu \rightarrow e\gamma)$ for the PMNS case in mSUGRA (red) and NUHM (green), and for the CKM case (blue) for $\tan\beta=10$ (left), for $\tan\beta=40$ (right). The different horizontal and vertical lines correspond to present and future limits on the respective observables.

present work, we have computed the $\mu \rightarrow e$ conversion rate in Titanium. The conversion rate is as usual normalized by the capture rate of the muon by the nucleus.

In figure 6, we present our results for $\text{CR}(\mu \rightarrow e \text{ in Ti})$ with respect to $\mu \rightarrow e + \gamma$. We find that there is a significant spread in the parameter space. This spread is due to the existence of cancellations between the penguin contributions at low $M_{1/2}$ and in low $\tan\beta$ regions, which has been noted earlier in the literature [33]. Still, we can see that the future experiments will be able to test most of the PMNS parameter space and will start to constrain the small-mixing scenario (CKM case).

The above plots have been obtained for the Titanium Nuclei. As in the case of $\mu \rightarrow eee$, it has been noted that the dominant contributions are from the dipole operators. In such a limit, where only the dipole operators contribute, one can easily estimate the conversion rate for the new nuclei, X, by knowing its effective charge, Z_{eff} , the form factor $F(q)$ and the atomic number Z and multiplying the conversion rates presented in the above plots by the ratio:

$$R = \frac{\left[Z_{eff}^4 |F(q)|^2 Z \right]_X}{\left[Z_{eff}^4 |F(q)|^2 Z \right]_{\text{Ti}}} \quad (4.3)$$

The Form factors and Z_{eff} for various Nuclei can be found in [54].

4.1 Combined effect of the Higgs mass and $\text{BR}(\mu \rightarrow e\gamma)$ bounds

Given the strong constraints from both $\text{BR}(\mu \rightarrow e\gamma)$ and the light Higgs mass one would wonder how much of the total parameter space from eq. (3.1) survives in the PMNS case. In figure 7 we plot the lightest Higgs mass as a function of m_0 , $M_{1/2}$, A_0 and $\tan\beta$ in the three left (right) panels for the mSUGRA (NUHM1) case. In particular, the left panel of the third row shows the asymmetric regions in A_0 required by the Higgs mass range.⁵ Flavor constraints instead are approximately symmetric in A_0 . The last row in the left panel shows the constraint on $\tan\beta$. As we can see in the mSUGRA case both low $\tan\beta$ ($\lesssim 5$) and high $\tan\beta$ ($\gtrsim 20$) are ruled out. The constraints in the low $\tan\beta$ are due to m_h whereas those at high $\tan\beta$ are from $\text{BR}(\mu \rightarrow e\gamma)$.

⁵We remind that the gluino-driven radiative effects gives a negative contribution to the stop A-term A_t , so that, if $A_0 > 0$ only very large values could still provide a sizeable $|A_t|$ at low energy.

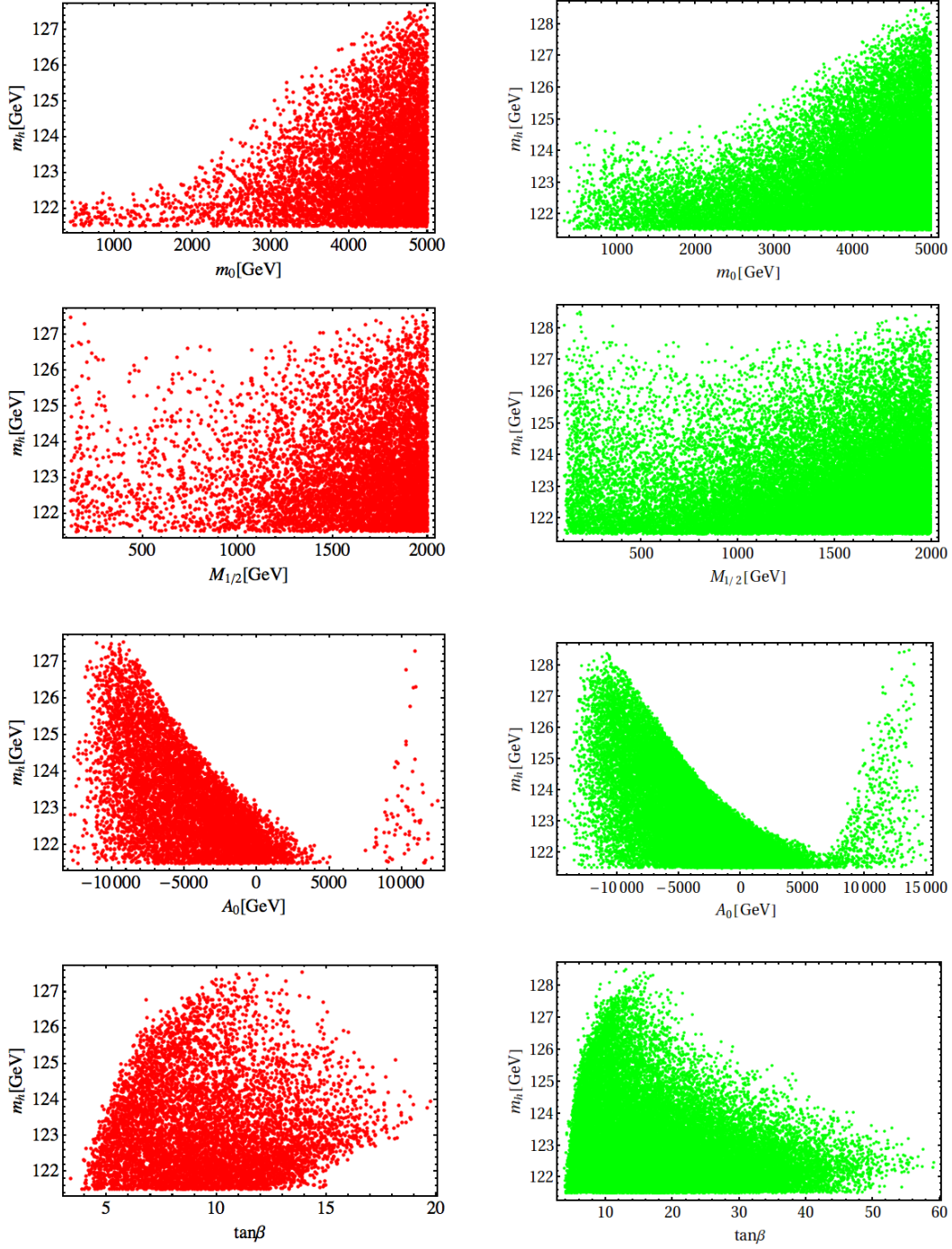


Figure 7. Here we present combined regions of parameter space allowed by $\text{BR}(\mu \rightarrow e\gamma)$ and the light Higgs mass (m_h), eq. (3.2), on the PMNS case in mSUGRA and NUHM1.

In mSUGRA/CMSSM models, a light Higgs mass around ~ 125 GeV requires either very heavy stops ($\tilde{t}_{1,2}$) ~ 4 TeV or a large stop mixing triggered by a large low-energy value of the stop A -term, $|A_t|$. In either of these cases, one can easily convince oneself,

using eq.(2.2) that the flavor violating parameter $\left(\delta_{i \neq j}^\ell\right)_{LL}$ is not suppressed. Thus a light Higgs mass ~ 125 GeV does not necessarily mean a suppressed flavor violating entry in spite of the largeness of stops ($\tilde{t}_{1,2}$) or A -terms required. In fact flavor violation constraints are still very strong.

In NUHM1 case this correlation is somewhat lost due to partial cancellation in the flavor violating entry⁶. All values of $\tan\beta$ are now allowed and A_0 is slightly more symmetric compared to the mSUGRA case. The surprising thing is that imposing the light Higgs mass constraint restricts the parameter space to be within the reach of MUSIC and Project-X proposals.

5 Summary and Outlook

The discovery of a Higgs-like boson at the LHC with a mass close to 125 GeV is one of the most significant achievements in particle physics of all times. In the present work, we assumed that the particle seen at the LHC is the lightest neutral Higgs scalar of the MSSM. We then studied the implications of the observed mass range on SUSY seesaw models along with recent improvements in $\text{BR}(\mu \rightarrow e + \gamma)$ and measurements of θ_{13} . We looked at Type I seesaw model assuming SO(10) relations between the top Yukawa and the heaviest RH neutrino Dirac mass. We assuming two extreme cases of mixing to be present in the Dirac Yukawa matrix (a) small CKM like mixing and (b) PMNS like mixing.

We find that there is a strong complementarity in the PMNS case between the light higgs mass constraint and $\text{BR}(\mu \rightarrow e + \gamma)$. The lower $\tan\beta$ regions are strongly constrained by the recent measurement of the light Higgs mass and high $\tan\beta$ regions by present limit of MEG. What is surprising is that $\tan\beta > 20$ is already ruled out.

The NUHM1 boundary conditions is one more interesting framework where the interplay between the light Higgs mass constraint and the LFV constraints comes to play. To relax the LFV constraints one would need strong cancellations in the flavor violating entry, however regions with large cancellations are not favored by a light Higgs mass of around 125 GeV. Partial cancellations are however allowed which put these regions within the reach of MEG (Project X) for $\mu \rightarrow e\gamma$ ($\mu \rightarrow eee$).

Acknowledgments

AM would like to acknowledge support from the MIUR PRIN project ‘‘Matter-Antimatter Asymmetry, Dark Matter and Dark Energy in the LHC Era’’ and the EU project ‘‘Unification in the LHC Era’’ contract PITN-GA-2009-237920 (UNILHC). SKV thanks INFN, Padova section and Dipartimento di Fisica ‘Galileo Galilei’, University of Padova, for supporting his visit. He also thanks DST Ramanujan Fellowship SR/S2/RJN-25/2008 of Government of India for support. LC and KMP are grateful to CHEP, IISc for hospitality and support during their visits. KMP also thanks Anjan S. Joshipura for partial support for this visit.

A Description of Future Experiments and Prospects: Circa 2020

PRISM [57, 59] or Phase Rotated Intense Slow Muon source is an upcoming facility at J-PARC. It will accelerates muon beam using a magnetic field inside a muon storage ring

⁶In NUHM1 case the cancellations are constrained by the parameter choice of eq.(3.1).

LFV process	Experiment	Future limits	Year (expected)
BR($\mu \rightarrow e\gamma$)	MEG [8]	$\mathcal{O}(10^{-13})$	~ 2013
	Project X [55]	$\mathcal{O}(10^{-15})$	> 2021
BR($\mu \rightarrow eee$)	Mu3e [56]	$\mathcal{O}(10^{-15})$	~ 2017
	"	$\mathcal{O}(10^{-16})$	> 2017
	MUSIC [57]	$\mathcal{O}(10^{-16})$	~ 2017
	Project X [55]	$\mathcal{O}(10^{-17})$	> 2021
CR($\mu \rightarrow e$)	COMET [57]	$\mathcal{O}(10^{-17})$	~ 2017
	Mu2e [58]	$\mathcal{O}(10^{-17})$	~ 2020
	PRISM/PRIME [57, 59]	$\mathcal{O}(10^{-18})$	~ 2020
	Project X [55]	$\mathcal{O}(10^{-19})$	> 2021
BR($\tau \rightarrow \mu\gamma$)	Belle II [60]	$\mathcal{O}(10^{-8})$	> 2020
BR($\tau \rightarrow \mu\mu\mu$)	Belle II [60]	$\mathcal{O}(10^{-10})$	> 2020
BR($\tau \rightarrow e\gamma$)	Super B [45]	$\mathcal{O}(10^{-9})$	> 2020
BR($\tau \rightarrow \mu\gamma$)	Super B [45]	$\mathcal{O}(10^{-9})$	> 2020
BR($\tau \rightarrow \mu\mu\mu$)	Super B [45]	$\mathcal{O}(10^{-10})$	> 2020

Table 3. Future sensitivities of next-generation experiments.

and will deliver 10^{12} μ /second at an energy of few 10s of MeV. PRIME [57, 59] is a $\mu - e$ conversion detector for PRISM designed to stop clumps of μ in a thin foil, having an energy of about 20 MeV. Because of high monochromaticity, large pulse rate and very low background level it would reach a sensitivity of detecting branching ratios of ($\mu \rightarrow e$) conversion in nuclei around 10^{-18} within few years of running. The PRIME will improve the sensitivities to $\mu - e$ conversions by two orders of magnitude compared to the next-generation experiment COMET (Coherent Muon to Electron Transition) experiment.

Project X [55], proposed at Fermilab, is a next-generation experiment which has the potential to deliver very high power unprecedentedly intense μ -beams for precise measurements of the rare muon decays. Project X will use 0.5 MW beam of μ accelerated at 3 GeV which will be generated from high-power primary proton beam. With such an intense continuous muon beam, Project X can look for $\mu \rightarrow e\gamma$ with sensitivity of $\mathcal{O}(10^{-15})$ which is two order of magnitude improvement over the future reach of MEG. However, sensitivity below 10^{-15} appears beyond the reach of Project X unless innovative ideas regarding the detectors emerge. Like $\mu \rightarrow e\gamma$, searches for $\mu \rightarrow 3e$ also need continuous muon beam. Experiments at Project X will improve the sensitivity to $\mu \rightarrow 3e$ decays by at least three to four orders of magnitude, assuming significant efforts to develop new detector technologies. The Project X proposals for studying the $\mu - e$ conversion in nuclei are particularly interesting. Two distinct scenarios has been proposed. If the next-generation round of experiments (COMET and Mu2e) observe any signal of $\mu - e$ conversion, then the available muon beams at Project X would allow further precision studies with several $\mu - e$ events in different nuclei. If no signal of $\mu - e$ will be found in next-generation experiments, Project X could reach the sensitivities $\mathcal{O}(10^{-19})$ or beyond given some improvements in beam technologies. To achieve these goals, a proposal to use muon storage ring installed in the muon beam line is under consideration.

The Belle II [60] is an upgrade of the existing Belle detector at the KEK B-factory in Japan. It will make use of the upgraded Super KEKB accelerator. The Belle II detector

is expected to collect 40 times more luminosity ($8 \times 10^{35} \text{ cm}^{-2} \text{ s}^{-1}$) than the previous generation Belle detector and by 2022 it would collect an integrated luminosity of $\sim 50 \text{ ab}^{-1}$. The sensitivity for the τ two body decays is expected to improved by an order of magnitude.

Super B factory [45] is a proposed high luminosity electron-positron collider. With an integrated luminosity of 75 ab^{-1} , Super B would be able to explore a significant portion of parameter space of new physics scenarios by searching for LFV in τ decays. It is going to improve the sensitivities to different channels of τ decays by at least an order of magnitude or two. The future sensitivities of all these experiments are summarized in the table 3.

References

- [1] J. Incandela, “Talk given on July 4, 2012, CMS Collaboration.”
<http://indico.cern.ch/conferenceDisplay.py?confId=197461>.
- [2] F. Gianotti, “Talk given on July 4, 2012, ATLAS Collaboration.”
<http://indico.cern.ch/conferenceDisplay.py?confId=197461>.
- [3] P. P. Giardino, K. Kannike, M. Raidal, and A. Strumia, *Is the resonance at 125 GeV the Higgs boson?*, [arXiv:1207.1347](#).
- [4] J. Ellis and T. You, *Global Analysis of the Higgs Candidate with Mass 125 GeV*, [arXiv:1207.1693](#).
- [5] J. Espinosa, C. Grojean, M. Muhlleitner, and M. Trott, *First Glimpses at Higgs’ face*, [arXiv:1207.1717](#).
- [6] D. Carmi, A. Falkowski, E. Kuflik, T. Volansky, and J. Zupan, *Higgs After the Discovery: A Status Report*, [arXiv:1207.1718](#).
- [7] A. Parker, “SUSY Searches (ATLAS/CMS): the Lady Vanishes.”
<https://indico.cern.ch/contributionDisplay.py?contribId=11&confId=181298>, 2012.
- [8] **MEG collaboration** Collaboration, J. Adam *et. al.*, *New limit on the lepton-flavour violating decay $\mu^+ \rightarrow e^+ \gamma$* , *Phys.Rev.Lett.* **107** (2011) 171801, [[arXiv:1107.5547](#)].
- [9] **DAYA-BAY Collaboration** Collaboration, F. An *et. al.*, *Observation of electron-antineutrino disappearance at Daya Bay*, *Phys.Rev.Lett.* **108** (2012) 171803, [[arXiv:1203.1669](#)].
- [10] **RENO collaboration** Collaboration, J. Ahn *et. al.*, *Observation of Reactor Electron Antineutrino Disappearance in the RENO Experiment*, *Phys.Rev.Lett.* **108** (2012) 191802, [[arXiv:1204.0626](#)].
- [11] L. J. Hall, D. Pinner, and J. T. Ruderman, *A Natural SUSY Higgs Near 126 GeV*, *JHEP* **1204** (2012) 131, [[arXiv:1112.2703](#)].
- [12] S. Heinemeyer, O. Stal, and G. Weiglein, *Interpreting the LHC Higgs Search Results in the MSSM*, *Phys.Lett.* **B710** (2012) 201–206, [[arXiv:1112.3026](#)].
- [13] A. Arbey, M. Battaglia, and F. Mahmoudi, *Constraints on the MSSM from the Higgs Sector: A pMSSM Study of Higgs Searches, $B_s^0 \rightarrow \mu^+ \mu^-$ and Dark Matter Direct Detection*, *Eur.Phys.J.* **C72** (2012) 1906, [[arXiv:1112.3032](#)].
- [14] A. Arbey, M. Battaglia, A. Djouadi, F. Mahmoudi, and J. Quevillon, *Implications of a 125 GeV Higgs for supersymmetric models*, *Phys.Lett.* **B708** (2012) 162–169, [[arXiv:1112.3028](#)].
- [15] P. Draper, P. Meade, M. Reece, and D. Shih, *Implications of a 125 GeV Higgs for the MSSM and Low-Scale SUSY Breaking*, *Phys.Rev.* **D85** (2012) 095007, [[arXiv:1112.3068](#)].
- [16] M. Carena, S. Gori, N. R. Shah, and C. E. Wagner, *A 125 GeV SM-like Higgs in the MSSM and the $\gamma\gamma$ rate*, *JHEP* **1203** (2012) 014, [[arXiv:1112.3336](#)].

- [17] N. D. Christensen, T. Han, and S. Su, *MSSM Higgs Bosons at The LHC*, [arXiv:1203.3207](#).
- [18] H. Baer, V. Barger, and A. Mustafayev, *Implications of a 125 GeV Higgs scalar for LHC SUSY and neutralino dark matter searches*, *Phys.Rev.* **D85** (2012) 075010, [[arXiv:1112.3017](#)].
- [19] M. Kadastik, K. Kannike, A. Racioppi, and M. Raidal, *Implications of the 125 GeV Higgs boson for scalar dark matter and for the CMSSM phenomenology*, *JHEP* **1205** (2012) 061, [[arXiv:1112.3647](#)].
- [20] O. Buchmueller, R. Cavanaugh, A. De Roeck, M. Dolan, J. Ellis, *et. al.*, *Higgs and Supersymmetry*, [arXiv:1112.3564](#).
- [21] L. Aparicio, D. Cerdeno, and L. Ibanez, *A 119-125 GeV Higgs from a string derived slice of the CMSSM*, *JHEP* **1204** (2012) 126, [[arXiv:1202.0822](#)].
- [22] J. Ellis and K. A. Olive, *Revisiting the Higgs Mass and Dark Matter in the CMSSM*, *Eur.Phys.J.* **C72** (2012) 2005, [[arXiv:1202.3262](#)].
- [23] H. Baer, V. Barger, and A. Mustafayev, *Neutralino dark matter in mSUGRA/CMSSM with a 125 GeV light Higgs scalar*, *JHEP* **1205** (2012) 091, [[arXiv:1202.4038](#)].
- [24] M. Hirsch, F. Joaquim, and A. Vicente, *Constrained SUSY seesaws with a 125 GeV Higgs*, [arXiv:1207.6635](#).
- [25] A. Masiero, S. K. Vempati, and O. Vives, *Seesaw and lepton flavor violation in SUSY SO(10)*, *Nucl.Phys.* **B649** (2003) 189–204, [[hep-ph/0209303](#)].
- [26] L. Calibbi, A. Faccia, A. Masiero, and S. Vempati, *Lepton flavour violation from SUSY-GUTs: Where do we stand for MEG, PRISM/PRIME and a super flavour factory*, *Phys.Rev.* **D74** (2006) 116002, [[hep-ph/0605139](#)].
- [27] L. Calibbi, R. Hodgkinson, J. Jones-Perez, A. Masiero, and O. Vives, *Flavour and Collider Interplay for SUSY at LHC7*, *Eur.Phys.J.* **C72** (2012) 1863, [[arXiv:1111.0176](#)].
- [28] J. R. Ellis, T. Falk, K. A. Olive, and Y. Santoso, *Exploration of the MSSM with nonuniversal Higgs masses*, *Nucl.Phys.* **B652** (2003) 259–347, [[hep-ph/0210205](#)].
- [29] A. Masiero, S. K. Vempati, and O. Vives, *Massive neutrinos and flavor violation*, *New J.Phys.* **6** (2004) 202, [[hep-ph/0407325](#)].
- [30] A. Masiero, S. Vempati, and O. Vives, *Flavour physics and grand unification*, [arXiv:0711.2903](#).
- [31] F. Borzumati and A. Masiero, *Large Muon and electron Number Violations in Supergravity Theories*, *Phys.Rev.Lett.* **57** (1986) 961.
- [32] J. Casas and A. Ibarra, *Oscillating neutrinos and $\mu \rightarrow e, \gamma$* , *Nucl.Phys.* **B618** (2001) 171–204, [[hep-ph/0103065](#)].
- [33] J. Hisano, T. Moroi, K. Tobe, and M. Yamaguchi, *Lepton flavor violation via right-handed neutrino Yukawa couplings in supersymmetric standard model*, *Phys.Rev.* **D53** (1996) 2442–2459, [[hep-ph/9510309](#)].
- [34] E. Arganda, M. Herrero, and A. Teixeira, *μ -e conversion in nuclei within the CMSSM seesaw: Universality versus non-universality*, *JHEP* **0710** (2007) 104, [[arXiv:0707.2955](#)].
- [35] D. Chowdhury, R. Garani, and S. K. Vempati, *SUSEFLAV: Program for supersymmetric mass spectra with seesaw mechanism and rare lepton flavor violating decays*, [arXiv:1109.3551](#).
- [36] F. E. Paige, S. D. Protopopescu, H. Baer, and X. Tata, *ISAJET 7.69: A Monte Carlo event generator for pp, anti-p p, and e+e- reactions*, [hep-ph/0312045](#).
- [37] G. Degrandi, P. Slavich, and F. Zwirner, *On the neutral Higgs boson masses in the MSSM for*

- arbitrary stop mixing, *Nucl.Phys.* **B611** (2001) 403–422, [[hep-ph/0105096](#)].
- [38] A. Brignole, G. Degrossi, P. Slavich, and F. Zwirner, *On the $O(\alpha(t)^{**2})$ two loop corrections to the neutral Higgs boson masses in the MSSM*, *Nucl.Phys.* **B631** (2002) 195–218, [[hep-ph/0112177](#)].
 - [39] A. Dedes and P. Slavich, *Two loop corrections to radiative electroweak symmetry breaking in the MSSM*, *Nucl.Phys.* **B657** (2003) 333–354, [[hep-ph/0212132](#)].
 - [40] A. Dedes, G. Degrossi, and P. Slavich, *On the two loop Yukawa corrections to the MSSM Higgs boson masses at large $\tan\beta$* , *Nucl.Phys.* **B672** (2003) 144–162, [[hep-ph/0305127](#)].
 - [41] **Particle Data Group** Collaboration, K. Nakamura *et. al.*, *Review of particle physics*, *J.Phys.G* **G37** (2010) 075021.
 - [42] **LHCb collaboration** Collaboration, R. Aaij *et. al.*, *Strong constraints on the rare decays $B_s \rightarrow \mu^+\mu^-$ and $B^0 \rightarrow \mu^+\mu^-$* , [arXiv:1203.4493](#).
 - [43] **Heavy Flavor Averaging Group** Collaboration, D. Asner *et. al.*, *Averages of b -hadron, c -hadron, and τ -lepton Properties*, [arXiv:1010.1589](#).
 - [44] A. Arbey, M. Battaglia, A. Djouadi, and F. Mahmoudi, *The Higgs sector of the phenomenological MSSM in the light of the Higgs boson discovery*, [arXiv:1207.1348](#).
 - [45] J. Hewett, H. Weerts, R. Brock, J. Butler, B. Casey, *et. al.*, *Fundamental Physics at the Intensity Frontier*, [arXiv:1205.2671](#).
 - [46] **SINDRUM Collaboration** Collaboration, U. Bellgardt *et. al.*, *Search for the Decay $\mu^+ \rightarrow e^+e^+e^-$* , *Nucl.Phys.* **B299** (1988) 1.
 - [47] **SINDRUM II Collaboration.** Collaboration, C. Dohmen *et. al.*, *Test of lepton flavor conservation in $\mu^+ \rightarrow e^+$ conversion on titanium*, *Phys.Lett.* **B317** (1993) 631–636.
 - [48] M. Tortola, J. Valle, and D. Vanegas, *Global status of neutrino oscillation parameters after recent reactor measurements*, [arXiv:1205.4018](#).
 - [49] S. Antusch, E. Arganda, M. Herrero, and A. Teixeira, *Impact of θ_{13} on lepton flavour violating processes within SUSY seesaw*, *JHEP* **0611** (2006) 090, [[hep-ph/0607263](#)].
 - [50] L. Calibbi, A. Faccia, A. Masiero, and S. Vempati, *Running $U(e3)$ and $BR(\mu \rightarrow e + \gamma)$ in SUSY-GUTs*, *JHEP* **0707** (2007) 012, [[hep-ph/0610241](#)].
 - [51] G. Altarelli, F. Feruglio, L. Merlo, and E. Stamou, *Discrete Flavour Groups, θ_{13} and Lepton Flavour Violation*, [arXiv:1205.4670](#).
 - [52] J. Hisano, M. Nagai, P. Paradisi, and Y. Shimizu, *Waiting for $\mu \rightarrow e$ gamma from the MEG experiment*, *JHEP* **0912** (2009) 030, [[arXiv:0904.2080](#)].
 - [53] Y. Kuno and Y. Okada, *Muon decay and physics beyond the standard model*, *Rev.Mod.Phys.* **73** (2001) 151–202, [[hep-ph/9909265](#)].
 - [54] R. Kitano, M. Koike, and Y. Okada, *Detailed calculation of lepton flavor violating muon electron conversion rate for various nuclei*, *Phys.Rev.* **D66** (2002) 096002, [[hep-ph/0203110](#)].
 - [55] “Project X and the Science of Intensity Frontier: A White Paper.” <http://projectx.fnal.gov/>, 2009.
 - [56] A. Blondel *et. al.*, “Letter of Intent for an Experiment to Search for the Decay $\mu \rightarrow eee$.” http://www.psi.ch/mu3e/DocumentsEN/L01_Mu3e_PSI.pdf, 2011.
 - [57] Y. Kuno, *Muon to electron conversion experiment*, *Nucl.Phys.Proc.Suppl.* **217** (2011) 337–340.
 - [58] “The Mu2e Conceptual Design Report 2012.” <http://mu2e-docdb.fnal.gov/cgi-bin/ShowDocument?docid=1169>, 2012.

- [59] R. Barlow, *The PRISM/PRIME project*, *Nucl.Phys.Proc.Suppl.* **218** (2011) 44–49.
- [60] T. Aushev, W. Bartel, A. Bondar, J. Brodzicka, T. Browder, *et. al.*, *Physics at Super B Factory*, [arXiv:1002.5012](#).